Journal of Water Process Engineering 25 (2018) 15–21

Contents lists available at ScienceDirect

Journal of Water Process Engineering

journal homepage: www.elsevier.com/locate/jwpe

Robust nanocatalyst membranes for degradation of atrazine in water

H. Vijwani, M.N. Nadagouda, S.M. Mukhopadhyay*

Center for Nanoscale Multifunctional Materials, Mechanical & Materials Engineering, Wright State University, Dayton, OH 45435, United States

ARTICLE INFO

Keywords:
Hierarchical hybrid surfaces as catalyst support
Carbon nanotube carpets on porous membranes
Palladium nano-particles
Atrazine degradation
Surface chemical states
Nano-catalysts

ABSTRACT

Solid membranes for degradation of emerging contaminants such as atrazine is of significant interest for water engineering applications. In this study, nanocatalyst particles have been anchored on vertically-aligned carpet-like arrays of carbon nanotubes (CNT) grown on porous carbon foams. This hierarchical architecture combines the advantages of highly surface-active nanoparticles with the robust and reusable structural advantage of porous solid membranes suitable for water treatment devices. Three types of palladium-based nano-catalytic surfaces have been investigated: metallic palladium (Pd), Pd nanoparticle with a layer of oxide (PdO-coated Pd), and Pd nanoparticle coated with thin film of silver (Ag-Pd). Their catalytic activities have been compared by analysing the degradation rate of atrazine in water. It is noted that all three catalysts show high levels of atrazine degradation, with the PdO-coated nanoparticles showing the highest kinetics. These results demonstrate that hierarchical hybrid architectures can provide compact and powerful surface-active materials such as adsorbents and catalytic degradation devices in future water treatment applications.

1. Introduction

A wide variety of pollutants have been identified by the United States Environmental Protection Agency (USEPA) as contaminants of emerging concern (CECs) in water, which pose potential threat to environment and public health [1–5]. These come from common industrial products such as detergents, pharmaceuticals, antimicrobial agents, plasticizers, fertilizers, herbicides, and pesticides. Specific compounds include atrazine, bisphenol-A, triclosan, triclocarban, perfluorooctanoic acid, octylphenol, nonylphenol, carbamazepine, and progestron, which can be present in ground water as well as in treated wastewater effluents released into waterways. There is significant need for sustainable and viable approaches of removing, preferable degrading, these contaminants. Potential techniques investigated include adsorption, ozonation, bio-reduction, photo-degradation, electro-catalytic and catalytic methods [6–15].

For any reaction involving heterogeneous catalysts, the available surface area for active catalytic sites and their structural/chemical/electronic states are important variables to consider. It is well-recognized that nanoscale catalysts can provide significant improvements over conventional solids due to their high surface/volume ratios and high chemical activities. However, the widespread use of nanomaterials is limited in real-life applications because of challenges related to their environmental proliferation, reusability, recovery and safety. These issues can be addressed by anchoring catalytic nanoparticles on larger solids, in which case the available surface area of nanocatalyst may be significantly constrained by the morphology of the underlying solid. Our research group has extensively investigated how these limitations can be overcome by durable attachment of functional nanoparticles on bio-mimetic hierarchical membranes that can pack exceptionally high density of surface active nano-catalytic particles into compact space, which can be safely deployed in flowing water [16–22]. A very effective architecture for aqueous environments is a high porosity foam made of inert carbon, which is enriched with strongly anchored carpets of carbon nanotubes that are, in turn, activated with selected catalytic nanoparticles.

In this study, we have used this architecture to build three types of palladium-based nano-catalysts. These have been used to degrade a model emerging contaminant, atrazine. Atrazine, chemically known as 6-chloro-N-ethyl-N'-(1-methylethyl)-1,3,5-triazine-2,4-diamine or 2-Chloro-4-ethylamino-6-isopropylamino-1,3,5-triazine, has a chemical formula of $C_8H_{14}ClN_5$ and a molecular weight of 215.1. Its solubility in water at 20 °C is 30 mg/L. It is a triazine herbicide that inhibits photosynthetic electron transport and is commonly used for controlling the growth of weed on various crops such as wheat, sugarcane, guava, corn, sorghum and a wide range of grasses. It is widely used in the United States, maybe about 64–75 million pounds per year [23,24]. As an herbicide, atrazine is directly applied to the soil during the pre-planting process and, due to its solubility in water, it can easily migrate into the ground and surface waters. Moreover, it has very low natural biodegradability, and persists in the environment once introduced. Due to its potential ecological and health effects, the USEPA has recommended

* Corresponding author.
E-mail address: smukhopa@wright.edu (S.M. Mukhopadhyay).

https://doi.org/10.1016/j.jwpe.2018.05.016
Received 7 February 2018; Received in revised form 24 May 2018; Accepted 28 May 2018

that the maximum contamination level of atrazine in drinking water should not exceed 3 µg/L or ppb [24,25].

The adsorption of atrazine on adsorbents is not very effective due to its low adsorption ability. It is therefore of interest to treat it using biological, oxidative/reductive, or catalytic techniques, as reported by earlier investigators [10–15]. Reducing agents reported include photocatlytic oxides, zerovalent iron (ZVI), and palladium [10,11,13]. There have been an earlier report [10] of Pd catalyst on polypyrrole-coated cellulose fibers tested on various contaminants in aerobic conditions. It was shown that while some of the other contaminants could be degraded, atrazine was extremely persistent in aerobic conditions. Investigations on electro-catalytic hydrogen-dehalogenation of atrazine using Pd-containing bimetallic catalysts [14] indicate need for certain threshold currents.

In this paper, we have investigated the possibility of using Pd-based nanocatalysts in robust reusable structures to degrade atrazine without any electric field or light activation. Three Nanoparticles tested are: pure metallic palladium (Pd-NPs), palladium oxide coated Pd (PdO-NPs), and silver-coated palladium (Ag/Pd-NPs), each supported on hierarchical carbon supports in the presence of hydrogen (anaerobic conditions). Structural and chemical properties of the hierarchical solid material were investigated using Field Emission Scanning Electron Microscopy (FE-SEM) and X-ray Photoelectron Spectroscopy (XPS) respectively. Liquid chromatography – Mass Spectroscopy (LC–MS) techniques were used to analyse the degradation kinetic rates and intermediate products formed during degradation.

2. Experimental

2.1. Materials and chemicals

The chemical reagents used in this study were of analytical grade and consumed without further purification. These include atrazine ($C_8H_{14}ClN_5$, Sigma Aldrich, Fluka Analytical Pesternal® Analytical Standard 45330), d_5-atrazine ($C_8H_9D_5ClN_5$, Sigma Aldrich, Fluka Analytical Pesternal® Analytical Standard) and 2-propanol (99.9%, HPLC Grade, Fisher Scientific). Teflon-lined butyl rubber stoppers (PTFE-lined) of size 20 mm and aluminium crimp were purchased from Wheaton Inc, and PTFE syringe filters (Supelco©) were used. Other materials include de-ionized water (DI water) and laboratory grade gases that include 5% H_2 balance N_2. The atrazine stock solution of 100 µg/mL concentration was prepared by dissolving 5 mg of atrazine in 50 mL methanol.

2.2. Fabrication of substrates and nano-catalysts

The substrates used in this study are carpet-like arrays of vertically aligned carbon nanotubes (CNT) grown on the surfaces of carbon foam (reticulated vitreous carbon or RVC foams provided by Ultramet). CNT arrays are grown using a two-step technique discussed in earlier publications (16–17). The first step involves microwave plasma deposition of silica film on the porous foam surface. This is followed by thermal chemical vapour deposition (CVD) of carbon nanotube arrays using floating catalyst technique.

These CNT-coated foams are used as supports to grow palladium nanoparticles (Pd-NP) using liquid-phase synthetic approach elaborated in earlier papers [18,19]. This technique involves soaking the CNT-coated substrate in tetra-amine palladium solution, and subsequently heat-treating in three stages: (i) Drying at 100 °C, (ii) Calcination at 400 °C in oxygen deficient inert atmosphere (Ar), and (iii) Final reduction and annealing at 450 °C in reducing environment containing hydrogen in Ar as the carrier gas. This produces base metallic Pd, with average particle size of 10–15 nm. The palladium-oxide coated nanoparticles were prepared by thermally oxidizing the Pd-NPs by heating them in ambient environment at 250 °C for 2 h. The Ag-Pd bimetallic nanoparticles were fabricated by taking the base Pd-CNT-Foam materials and subsequently depositing silver films on them using a liquid phase approach. Deposition of silver was done by infiltrating the CNT-foam supported Pd-NP s with AgNO3 precursor solution and subsequently heating them at 40 °C using dimethyl siloxane (DMS) as reducing agent and sodium citrate as capping agent. More details of the Ag coating process are available in earlier publication [20].

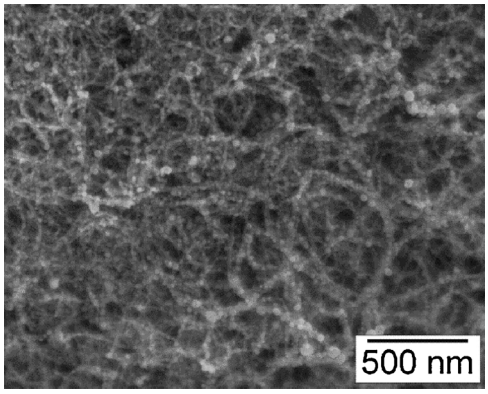

Fig. 1. SEM micrograph of palladium nanoparticles (Pd-NPs) fabricated on CNT-coated RVC foams.

2.3. Batch degradation studies

Catalytic materials compared in this study are (i) RVC foam, (ii) CNT-RVC foam, (iii) Pd-CNT-RVC foam, (iv) PdO-CNT-RVC foam, and (v) Ag-Pd on CNT-RVC foam. They were tested in batch reactors consisting of 160 mL glass serum bottles. The palladium-based catalyst supports (Pd-CNT, PdO-CNT, and Ag-Pd CNT on RVC foams), were rinsed in 2-propanol and water. Subsequently, two samples, each of size Ø 8 mm x 5 mm and total weight ~ 25 mg (total of 50 mg of solid, which contains about 0.15-0.16 mg of Pd) were attached to the inside wall of the serum bottle using double-sided carbon tape. Approximately 80 mL of 5% v/v methanol in Milli-Q water was added to the reactors, maintaining the solution to headspace ratio of 50:50. The pH was monitored using a pH meter every 20 min, and stayed within a slightly acidic range of 6.7-6.9. The reactors were sealed with Teflon-lined butyl rubber stoppers and aluminium crimps and then treated in two ways. In one set of experiments, they were sealed with ambient air. In another set, they were purged with high purity hydrogen-nitrogen mixture (5% H_2 and a balance N_2) for approximately 30 min. Atrazine stock solution was injected into each reactor (initial atrazine conc. = 1 µg mL^{-1} or 4.63 µM; initial atrazine amount = 0.463 µmol in 100 mL) using a gas-tight syringe. The reactors were then placed on an end-over-end rotary shaker at room temperature (60 rpm, 30° inclination). The bottles were placed on the rotator at an inclination such that the solid samples attached on the walls of the reactors remained immersed in liquid-phase at all times during rotation. A blank reactor without any support or catalyst material was also investigated.

Aliquot samples of 2 mL were derived from the bottles using a syringe at specified time intervals (20 min). Samples collected in the syringe at different reaction times were filtered using disposable PTFE syringe filters. Initially, a 1 mL aliquot sample was discarded by running it through the filter in order to saturate the filter and then the remaining liquid sample was collected through the saturated filter in a 2 mL vial for HPLC analysis.

2.3.1. Internal standard – d_5-atrazine

An internal standard was added to the aliquot samples collected in a 2 mL vial for high performance liquid chromatography (HPLC) quantification. In this study, a deuterated atrazine – 'd_5-atrazine' compound was used as an internal standard for atrazine analysis. Stock solution of d_5-atrazine was prepared to obtain the concentration 10 µg/mL in 65%

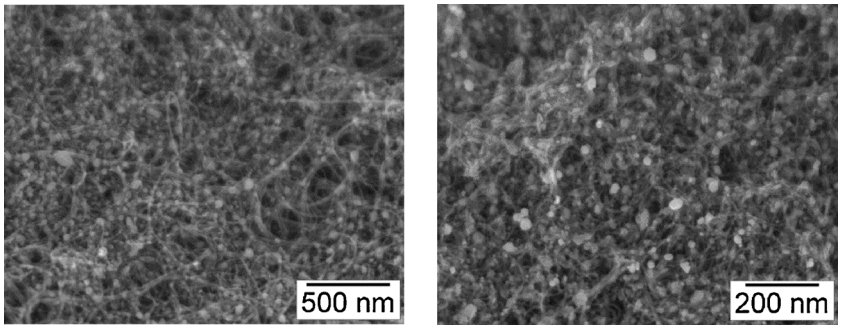

Fig. 2. SEM micrographs of (a) Pd-O, and (b) Ag-coated Pd-NPs synthesized on RVC-CNT hybrid foam structure samples.

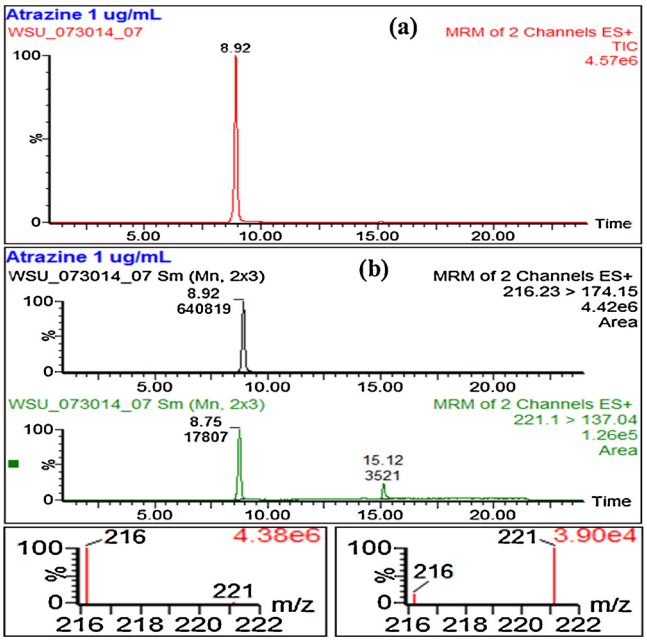

Fig. 3. A typical (a) full scan TIC chromatograph and (b) LC–MS/MS chromatogram acquired in multiple reaction monitoring mode for Atrazine (216.2) and d_5-Atrazine (221.1) ion channels.

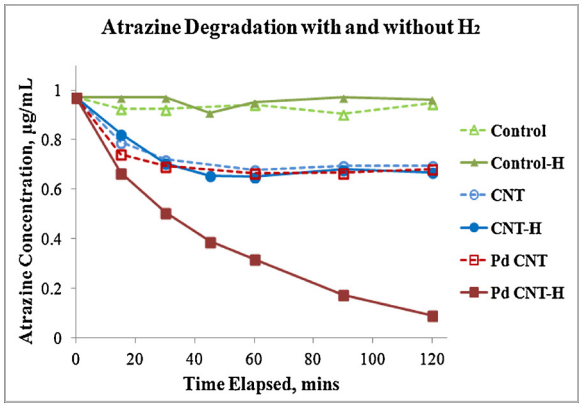

Fig. 4. Degradation kinetics of atrazine (initial concentration of 1 µg/mL) obtained for the control, CNT foam, and Pd-CNT foam reactor samples with and without H_2 gas purging. Dotted lines are reactions without H_2 purging.

(v/v) methanol and 2 mM acetic acid. 50 µL of d_5-atrazine stock solution (10 µg/mL) was carefully measured using an automatic micropipette and added to each vial having 1 mL solution. The concentration of internal standard in each vial was maintained at 0.5 µg/mL.

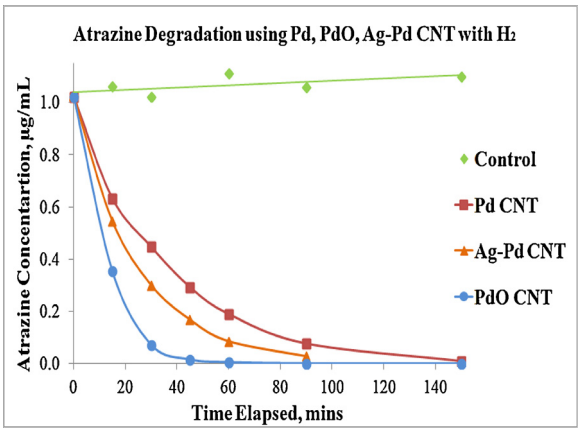

Fig. 5. Degradation kinetics of atrazine (initial concentration of 1 µg/mL) obtained for the Pd-CNT, PdO-CNT, and bimetallic Ag-Pd CNT foam samples with H_2 gas purging (5% H_2 balance N_2) for 30 min.

2.3.2. Standard concentration analysis

For analytical purposes, a standard concentration of atrazine was studied for concentrations ranging from 0.01 µg/mL to 1 µg/mL (ppm). The standard solutions were prepared in 10 mL vials by adding the appropriate amount of atrazine stock solution in 5% (v/v) methanol in Milli-Q water. 1 mL solution from each standard was collected in small vials and a known amount of internal standard was added to this for quantitative HPLC analysis.

2.3.3. Chemical analysis – HPLC

Atrazine in water was analysed by using a Waters Micromass Quattro Micro equipped with a mass spectrometer for liquid chromatography (LC–MS) and an auto-sampler. The HPLC column was a Restek Biphenyl Column – Pinnacle DB Biphenyl Column of dimensions 100 × 2.1 mm^2 (1.9 µm) and temperature was set to 50 °C. A mixture of water and methanol containing 2 mM acetic acid (NH_4OAc) was used as the mobile phase. The ratio of methanol to reagent water containing 2 mM acetic acid was maintained at 10:90 (v/v%) for atrazine analysis. The flow rate of the pump was set at 0.3 mL/min and the actual sample injection volume was 20 µL. Each run was conducted for 24 mins. The method detection limit for atrazine was 0.5 ng/mL. Selective ion reaction monitoring (SIR) was carried out for pure atrazine and the fragment ion spectra was used for MS/MS analysis. SIR for all possible metabolites of atrazine was carried out using analyte solution to determine their formation due to the degradation of atrazine. The liquid analyte samples were analysed in the multiple reaction mode (MRM) using the fragment ions spectra for MS/MS analysis of atrazine and the possible metabolite (daughter product) compounds.

The catalytic degradation of atrazine is known to produce various derivative (metabolite or daughter) products and possible pathways for atrazine degradation during hydrogenated and hydroxylated reactions

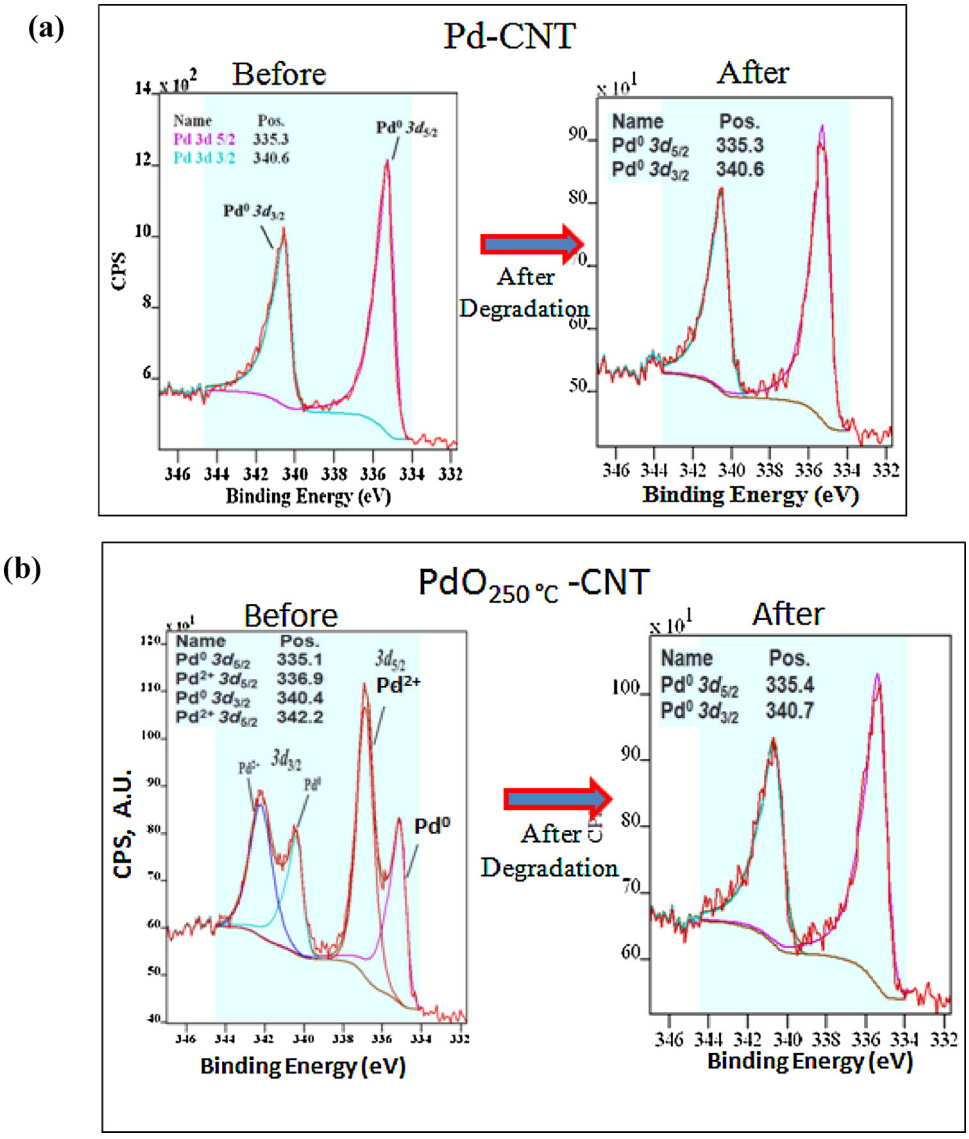

Fig. 6. XPS Pd 3d fine-scan spectra of before and after atrazine degradation using (a) Pd-CNT and (b) PdO-CNT on RVC foam.

are discussed in the literature [11–13]. In this study, daughter products from our samples were detected and quantified using LC–MS analysis, and possible degradation pathways proposed. An internal standard 'd_5-Atrazine' was used to quantify the peak intensities of the compounds in the HPLC analysis.

3. Results and discussions

3.1. Microstructure of the hierarchical catalytic materials

Fig. 1 depicts Scanning Electron Microscope (SEM) images of Pd-NPs deposited on CNT- foam supports. CNT-enrichment on the surface enables high loading of Pd nanoparticles in compact space. The SEM images show uniformly distributed Pd-NPs. Fig. 2(a) shows the palladium nanoparticles that were oxidized at 250 °C. Fig. 2(b) shows the microstructure of silver coated Pd nanoparticles (Ag-Pd) on CNT foam structures. These figures indicate that the distribution of nanoparticles are very similar in the three materials. The difference lies in surface chemical states, as discussed in the later section.

3.2. Atrazine degradation

Fig. 3 shows a typical total ion current (TIC) chromatogram acquired from the full scan mode in LC/MS and the graph shows the mass scan data collected over time. From this plot, the atrazine compound is obtained at retention time of ~8 mins using the above mentioned HPLC method.

Fig. 3b shows the multiple reaction monitoring (MRM) analysis modes that show the mass separation scan acquired in the MS experiment. The MRM peak acquired at 216.2 represents protonated atrazine – ionization (μ + 1) of atrazine and the MRM peak acquired at 221.1 represents protonated d_5-atrazine, ionization (μ + 1) of d_5-atrazine. The ratio of atrazine peak area to d_5-atrazine peak area is utilized here to control the run-to-run variability in injection and ionization intensity of HPLC. Similarly, other mass compounds were determined using SIR mode and acquired using MRM mode.

Calibration curves were obtained for every experiment from standard solution analysis by plotting the area ratios of atrazine and d_5-atrazine peaks with the known concentrations. The curve showed excellent linearity with the regression coefficient of $R^2 = 0.999$. This curve equation was used for determining the concentration of atrazine in the water samples.

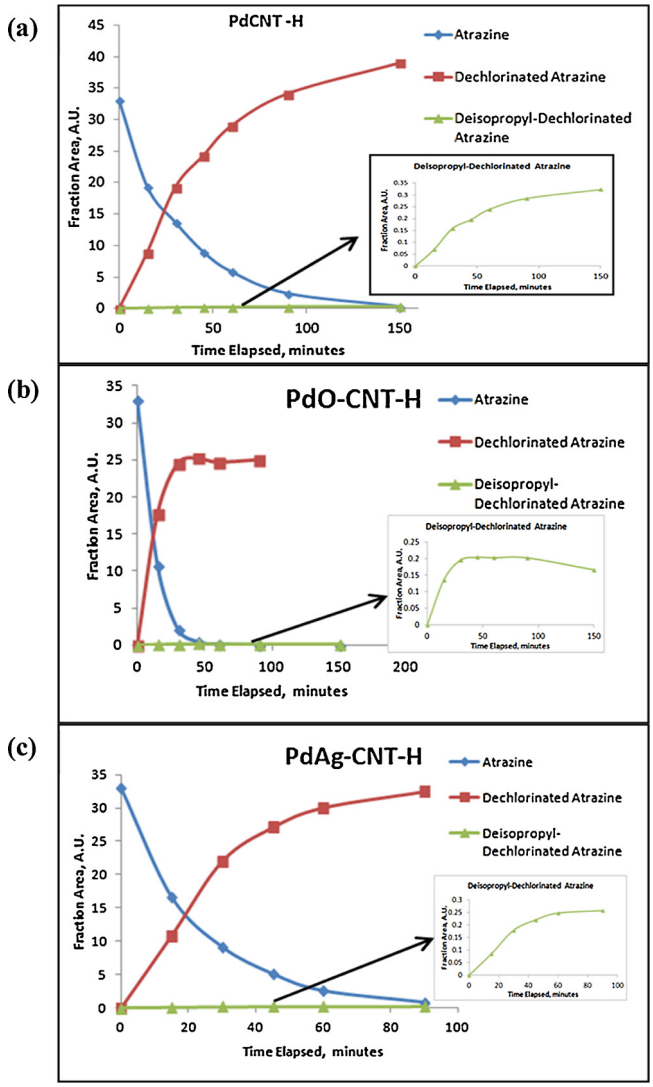

Fig. 7. Atrazine degradation and daughter product formation curves with (a) Pd-CNT Foam, (b) PdO-CNT Foam, and (c) Ag-Pd CNT Foam samples in the presence of hydrogen gas.

Fig. 4 shows the degradation kinetics of atrazine from an initial concentration of 1 µg/mL under two different conditions (with and without H2 purging) obtained from CNT foam, Pd-CNT foam, and control reactors. It is clear from Fig. 4 that the control reactor shows no significant degradation or removal of atrazine under any condition. For reactors containing CNT foam structures without H_2 purging, there is small but detectable amount of atrazine reduction (~30%). The Pd-CNT catalysts without H_2 show a similar effect of close to 30% atrazine removal. This reduction in concentration can be attributed to the adsorption of atrazine on the nanostructured surfaces (CNT and/or Pd-CNT). The base CNT-foam reactor with hydrogen but without Pd shows a similar removal rate as its non-H_2 counterpart, attributed to adsorption.

However, when samples decorated with Pd nano-catalysts are used in the presence of H_2, very noticeable reduction of atrazine is observed. This indicates that the presence of H_2 along with Pd nanocatalyst is needed to degrade the atrazine, which agrees with earlier reports in the literature [13,14]. The pH is important in atrazine degradation reactions, and was monitored periodically and observed to remain slightly acidic, in the 6.7-6.9 range.

Fig. 5 shows, with greater detail, the influence of surface chemical states of Pd NP on degradation kinetics of atrazine in the presence of H_2. It can be seen that each of the three catalysts investigated, Pd-CNT, PdO-CNT, and Ag-Pd CNT foam, show rapid degradation. Metallic Pd-CNT shows 50% degradation in about 25 mins and complete degradation in less than 120 mins. Oxide coated (PdO-CNT) and silver-coated (Ag-Pd CNT) samples show further increase in catalytic degradation rate, with the PdO nanoparticles being the fastest (50% degradation in 11.5 min, and complete degradation within 40 min). It is worth noting is that earlier studies that have compiled atrazine degradation rate by nanoparticles [13–15], including alloys containing Pd, have indicated much slower degradation rates. The fastest results [15] indicate incomplete removal (20% remaining) even after 12 h of treatment. While it is difficult to make quantitative comparisons in terms of Pd atomic sites available in each case, since such analyses are not available for earlier alloys, but it is absolutely clear that the robust hierarchical nanostructures of this study show very significantly improved atrazine degradation rates with complete reduction (below detection levels) in approximately 40, 80 and 120 min respectively. This underscores the future potential of these types of hierarchical hybrid design for nano-catalyst devices.

3.3. Surface chemical states of nanocatalysts before and after atrazine exposure

Detailed surface chemical analysis was performed on the nanoparticles using X-Ray Photoelectron Spectroscopy (XPS). XPS scans were performed before and after use in the reactor, in order to monitor any changes in surface chemistry during use. All samples (Pd, PdO, and Ag-Pd NPs on CNT-foam supports) were rinsed with methanol and water and allowed to dry for up to 48 h in air. The chemical state of metallic Pd-CNT samples for as-prepared and used catalyst is shown in Fig. 6a. The Pd 3d5/2 peak at 335.3 eV for Pd-CNT sample remains unchanged after atrazine degradation. Fig. 6b shows the fine scan of Pd 3d peak obtained from PdO250 °C sample before and after atrazine degradation. It can be observed that the partially oxidized PdO sample reduced to fully metallic state after degradation as the Pd 3d¬5/2 peak of Pd2+ at 336.9 eV shifts towards the 335.3 ± 0.1 eV, indicating release of surface oxide. For the Ag-Pd sample, the chemical states of both Ag and Pd in Ag-Pd CNT samples remained unchanged after atrazine degradation, hence not shown here.

3.4. Daughter products and proposed degradation pathways

Degradation products (daughter products) of atrazine in the presence of palladium-nanocatalysts and hydrogen with each nano-catalyst were monitored using Liquid Chromatography-Mass Spectroscopy (LCMS). Detectable daughter products observed are shown in Fig. 7. These include significant amounts of dechlorinated atrazine and deisopropyl-dechlorinated atrazine. In addition, trace amounts of de-ethyl-dechlorinated atrazine and de-ethyl-deisopropyl-dechlorinated atrazine were also detected (quantities too small to be quantified). This indicates that the degradation of atrazine yielded a dechlorinated atrazine compound as the major intermediate product in all cases; its increase correlating very well with decrease in atrazine concentration. Formation of trace amounts of further degradation products at the later stages indicates that, eventually, the dechlorinated atrazine would be further broken down to smaller molecules. Possible degradation mechanism has been proposed based on these results. Fig. 8 shows daughter products of atrazine when zero-valent Pd (Pd-NP and Ag-coated pd-NP) catalysts are used in the presence of H2. There may be more than one intermediate pathways, as indicated, but the most quantifiable degradation product observed is dechlorinated atrazine, which also agrees with the discussions in the literature [13]. Further reduction of dechlorinated atrazine to de-isopropyl-de-chlorinated atrazine was observed in trace amounts, which would finally lead to formation of “Guanmine” in trace amounts indicating to path 2 in Fig. 8 as one possible pathway. Additionally, traces of de-ethyl-de-chlorinated

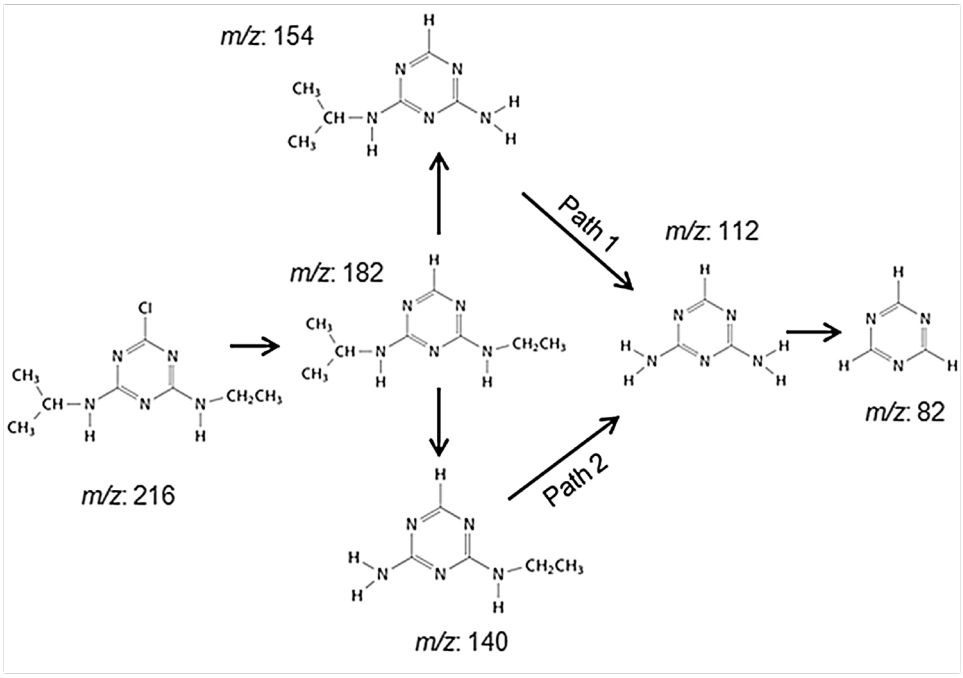

Fig. 8. Proposed mechanism for hydrogenated products of atrazine – catalytic degradation with palladium-based catalysts in the presence of hydrogen. Intermediate products seen were molecules of the de-chlorinated atrazine family, which are subsequently broken into smaller components.

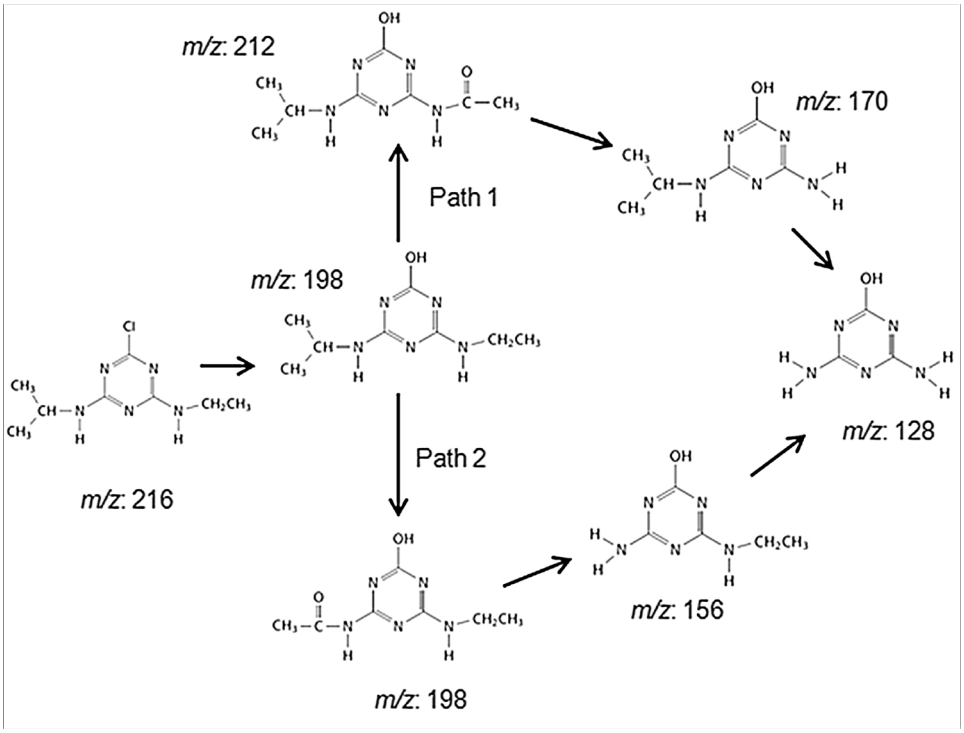

Fig. 9. Proposed mechanism of additional pathway when oxide coated palladium is used in the presence of hydrogen. Hydroxylated molecules of the atrazine family were detected along with those seen in Fig. 9.

atrazine were also observed, indicating some reduction through pathway 1. In summary zero-valent palladium NP in the presence of H_2 will cause atrazine to first reduce to dechlorinated-atrazine, followed by other products. The degradation mechanism presumably involves steps that include dissociative adsorption of reactant species on the surface of the Pd, chemical reaction between these intermediate adsorbed species forming the reduced product including HCl, and finally desorption of the final products from the catalyst surface and/or further degradation of the adsorbed intermediate species into the smaller daughter products.

The degradation mechanism of surface-oxidized PdO may involve additional pathways compared to metallic Pd-and Ag-Pd catalysts. It was observed that with PdO layer in the presence of H_2, the degradation of atrazine is significantly faster, and the prominent daughter product (dechlorinated atrazine) is smaller (Fig. 7c). This indicates that there will be additional degradation products such as hydroxylated atrazine

[12,13], which is further supported by the observation noted in the earlier section that the oxide layer from the PdO surface is removed after exposure to atrazine, resulting in reduced Pd after use. Based on these observations, it appears that of the nanoparticle surface has oxidized Pd, there may be additional breakdown mechanism(s) for atrazine through hydroxylated products as proposed in Fig. 9, in addition to the degradation mechanisms proposed in Fig. 9 to form dechlorinated atrazine.

4. Conclusions

In this study, Pd, PdO, and Ag-Pd on hierarchical carbon structures were used as catalysts in the presence of hydrogen gas for degradation of a model emerging contaminant, atrazine, in water. It was demonstrated that all three nanomaterials could completely degrade atrazine in water, without the need for electrical or optical stimuli. Among the three types of catalysts tested, PdO has the highest activity followed by Ag-Pd, and pure Pd nanoparticles. The atrazine initially transformed to form dechlorinated-atrazine and de-ethyl-deisopropyl-dechlorinated-atrazine. This architecture of catalyst particles attached to larger hierarchical carbon supports form durable hybrid solids that can be easily introduced in and out of water without detectable damage. Such structures may therefore provide a nonpolluting, reusable, and cost-effective solution for the removal of pollutants from contaminated water.

Acknowledgements

Financial support from the following programs are acknowledged: Ohio Third Frontier Program, National Science Foundation (CBET # 1747826), U.S. Environmental Protection Agency and Wright State University Ph.D. Fellowship.

References

[1] D.C. Wilson, T.L. Jones-Lepp, Emerging contaminant sources and fate in recharged treated wastewater, Lake Havasu city, Arizona, Environ. Eng. Geosci. 19 (2013) 231–251.
[2] USEPA, Occurrence of Contaminants of Emerging Concern in Wastewater From Nine Publicly Owned Treatment Works, EPA-821-R-09-009, U.S. Environmental Protection Agency Office of Water, 2009, p. 2009 (4303T).
[3] L. Schaider, J. Ackerman, R. Rudel, S. Dunagan, J. Brody, Emerging Contaminants in Cape Cod Private Drinking Water Wells, (2011).
[4] USEPA 2010 and EPA-820-R-10-002, Treating Contaminants of Emerging Concern – A Literature Review Database. U.S. Environmental Protection Agency Office of Water (4303T), 2010.
[5] R.N. Lerch, P.E. Blanchard, E.M. Thurman, Contribution of hydroxylated atrazine degradation products to the total atrazine load in midwestern streams, Environ. Sci. Technol. 32 (1998) 40–48.
[6] J. Li, Y. Zhan, J. Lin, A. Jiang, W. Xi, Removal of bisphenol A from aqueous solution using cetylpyridinium bromide (CPB)-modified natural zeolites as adsorbents, Environ. Earth Sci. 72 (10) (2014) 3969–3980.
[7] S.K. Behera, S.-Y. Oh, H.-S. Park, Sorption of triclosan onto activated carbon, kaolinite and montmorillonite: effects of pH, ionic strength, and humic acid, J. Hazard. Mater. 3 (July (1–3)) (2010) 684–691.
[8] S.H. Joo, D. Zhao, Destruction of lindane and atrazine using stabilized iron nanoparticles under aerobic and anaerobic conditions: effects of catalyst and stabilizer, Chemosphere 70 (3) (2008) 418–425.
[9] K. Chiang, T.M. Lim, L. Tsen, C.C. Lee, Photocatalytic degradation and mineralization of bisphenol A by TiO2 and platinized TiO2, Appl. Catal. A Gen. 261 (2) (2004) 225–237.
[10] M.N. Nadagouda, I. Desai, C. Cruz, D.J. Yang, Novel Pd based catalyst for the removal of organic and emerging contaminants, RSC Adv. 2 (2012) 7540–7548.
[11] T. Dombek, E. Dolan, J. Schultz, D. Klarup, Rapid reductive dechlorination of atrazine by zero-valent iron under acidic conditions, Environ. Pollut. 111 (2001) 21–27.
[12] R.N. Lerch, W.W. Donald, Analysis of hydroxylated atrazine degradation products in water using solid-phase extraction and high-performance liquid chromatography, J. Agric. Food Chem. 42 (4) (1994) 922–927.
[13] Sung Hee Joo, Dongye Zhao, Destruction of lindane and atrazine using stabilized iron nanoparticles under aerobic and anaerobic conditions: effects of catalyst and stabilizer, Chemosphere 70 (January (3)) (2008) 418–425.
[14] Y.L. Chen, L. Xiong, X.N. Song, W.K. Wang, Y.X. Huang, H.Q. Yu, Electrocatalytic hydrodehalogenation of atrazine in aqueous solution by Cu@Pd/Ti catalyst, Chemosphere 125 (April) (2015) 57–63, http://dx.doi.org/10.1016/j.chemosphere.2015.01.052 (Epub 2015 Feb 16).
[15] V.S. Susha, C.R. Chinnamuthu, Synthesis and characterization of iron based nanoparticles for the degradation of atrazine herbicide, Res. J. Nanosci. Nanotechnol. 2 (2012) 79–86.
[16] S.M. Mukhopadhyay, A. Karumuri, I.T. Barney, Hierarchical nanostructures by nanotube grafting on porous cellular surfaces, J. Phys. D: Appl. Phys. 42 (2009).
[17] I.T. Barney, D.S. Lennaerts, S.R. Higgins, S.M. Mukhopadhyay, Specific surface area of hierarchical graphitic substrates suitable for multifunctional applications, Mater. Lett. 88 (2012) 160–163.
[18] Hema Vijwani, Sharmila M. Mukhopadhyay, Palladium nanoparticles on hierarchical carbon surfaces: a new architecture for robust nano-catalysts applied surface science, Appl. Surf. Sci. 263 (2012) 712–721.
[19] Hema Vijwani, Abinash Agrawal, M. Sharmila Mukhopadhyay, Dechlorination of environmental contaminants using a hybrid nanocatalyst: palladium nanoparticles supported on hierarchical carbon nanostructure, J. Nanotechnol. 2012 (2012), http://dx.doi.org/10.1155/2012/478381 Article ID 478381.
[20] K. Anil Karumuri, P. Dhawal Oswalb, A. Heather Hostetlerand, M. Sharmila Mukhopadhyay, Silver nanoparticles attached to porous carbon substrates: robust materials for chemical-free water disinfection, Mater. Lett. 109 (October (15)) (2013) 83–87.
[21] Kshitij C. Jha, Zhuonan Liu, Hema Vijwani, Mallikarjuna Nadagouda, Sharmila M. Mukhopadhyay, Mesfin Tsige, Carbon nanotube based groundwater remediation: the case of Trichloroethylene, Molecules 21 (953) (2016), http://dx.doi.org/10.3390/molecules21070953.
[22] Elizabeth I. Maurer, Kristen K. Comfort, Saber M. Hussain, John J. Schlager, Sharmila M. Mukhopadhyay, Novel platform development using assembly of carbon nanotube, nanogold and immobilized RNA capture element for rapid, selective sensing of bacteria, Sensors 12 (2012) 8135–8144.
[23] USEPA, Revised Preliminary Human Health Risk Assessment: Atrazine. U.S. Environmental Protection Agency, Office of Pesticide Programs, (2001) (2001h Washington, D.C.).
[24] R. N. Brent, J. Schofield, K. Miller, and USEPA. 2001 EPA 905R-01-010., Results of the Lake Michigan Mass Balance Study: Atrazine Data Report December 2001, 2001.
[25] USEPA, National Primary Drinking Water Regulations, Contaminant Specific Fact Sheets, Synthetic Organic Chemicals, Technical Version. EPA 811/F-95/003-T., 1995, (1995).